Grazing-incidence antireflection films. IV. Application to Mössbauer filtering of synchrotron radiation

J. P. Hannon and G. T. Trammell
Physics Department, Rice University, Houston, Texas 77251

M. Mueller, E. Gerdau, R. Rüffer, and H. Winkler
II. Institute für Experimentalphysik, Universität D-2000 Hamburg 50, Federal Republic of Germany
(Received 9 May 1984; revised manuscript 28 January 1985)

In principle, a very bright, monochromatic 1-Å signal with $\hbar\Delta\omega\approx10^{-8}$—$10^{-6}$ eV can be filtered from white synchrotron radiation by multiple reflection at grazing incidence from mirrors coated with grazing-incidence antireflection (GIAR) films in which either the films or substrate contain resonant Mössbauer nuclei. Typically, nonresonant reflectivities can be suppressed to 10^{-4}—10^{-3} while maintaining resonant reflectivities of $\approx70\%$, with half-widths strongly broadened by "enhancement" to $\Gamma_{\rm eff}\approx20\Gamma$. Effective filtering should be possible with two to four reflections, or alternatively, with one to two reflections plus time resolution. By using different combinations of films and substrates, the response can be tailored to give narrow resonance widths $\Delta\omega\approx\Gamma$ and corresponding delayed scattering times to optimize time filtering, or at the other extreme, to produce broad-width filters with $\hbar\Delta\omega\approx100\Gamma$ which would be ideal for a high-resolution x-ray source. In the time response there will be "quantum beats" at frequencies Ω_B due to the interference between the radiation emitted by different hyperfine oscillators, so the beat pattern is determined by the hyperfine splitting. Also, there are two interesting dynamical effects—first, due to the "enchancement effect" the coherent decay is speeded up relative to the natural lifetime for incoherent decay and internal conversion absorption; and secondly, there will be "dynamical beats" at frequencies ω_B (superimposed on the quantum-beat spectrum) which is essentially an interference between the natural "ringing" of an oscillator at its resonsance frequency ω_0 and the collective response which rings with a median frequency $\omega_0+\omega_B$. Finally, there is also a multiple-reflection delay to the response, which should be a useful aid for time filtering. This paper develops the general theory for resonant filtering of synchrotron radiation using GIAR films, examining in particular the resulting frequency spectrum, the integrated response, and the time response for resonant ^{57}Fe mirrors coated with $\lambda/4$ GIAR filn

I. INTRODUCTION

In the preceding paper (paper III),[1] we developed the theory for pure nuclear reflections using grazing-incidence antireflection (GIAR) films to suppress the nonresonant electronic reflection. In this paper we apply this idea to the problem of Mössbauer filtering of synchrotron radiation.

Ruby[2] and Mössbauer[3] first pointed out that synchrotron sources can be so exceedingly bright in the 10-keV x-ray region that even within the highly monochromatic frequency region of a nuclear resonance width, $\hbar\Delta\omega\approx10^{-8}$ eV, the brightness can greatly exceed that available from natural γ-ray sources. Thus, in principle, using pure nuclear scattering, one can produce an "ultranarrow" bandpass filter to filter synchrotron radiation. The resulting beam will be highly monochromatic ($\hbar\Delta\omega\approx10^{-8}$—$10^{-6}$ eV) with a potential brightness greatly exceeding that available from other sources. Such a source would offer a unique high-resolution x-ray probe of "soft" inelastic excitations ($\hbar\Delta\omega\lesssim10^{-6}$ eV), opening up a new region inaccessible by other scattering methods. There will also be immediate application to Mössbauer experiments involving coherent scattering from perfect crystals, structure determination of biomolecules, and studies of surface magnetism. Also, the long coherence length of the signal (≈0.3—30 m) will open quite new possibilities in x-ray interferometry. Various aspects of the problem of filtering have been discussed by a number of authors.[2–12] Some initial positive results have been reported by Cohen[6] and Chechin *et al.*,[10] and the first definitive resonant signal has been obtained by Gerdau *et al.*[11]

Such filtering can be achieved by resonant scattering from the sharp Mössbauer transitions, making use of the unique features which distinguish the resonant nuclear scattering from the nonresonant electronic scattering—the slow scattering time, the sharp variation with frequency near resonance, and the sensitivity to crystalline electric and magnetic fields. Using these features, three main techniques have emerged to selectively scatter the resonant slice—(1) time-resolved scattering with detectors which are only turned on $\approx10^{-7}$ sec after each prompt synchrotron pulse to detect the slowly emitted resonant signal; (2) "superlattice" Bragg reflections from crystals with special magnetic or electric field symmetries which at special orientations will only scatter resonance radiation; and (3) grazing-incidence reflection from resonant mirror systems with antireflection films for suppressing

the nonresonant reflection.

The most extensive efforts have centered on using pure nuclear Bragg reflections,[4,5,7–11] in conjunction with time resolution, and the first successful filtering has been achieved using this method. Such resonant superlattice Bragg reflections offer the highest possible signal-to-noise ratio in a single reflection, and with a macroscopically perfect crystal it may even be possible to resonantly filter with a single superlattice reflection. However, there are several problems which arise, all centered on the severe restrictions imposed by the Bragg condition: (1) Most important is the problem of obtaining highly perfect single crystals which produce pure nuclear reflections (peak reflectivities and the signal-to-noise ratio are reduced by mosaic structure); (2) the narrow Bragg acceptance angles allow only a portion of the incident beam to be utilized (or for mosaic crystals or thin films which have acceptance angles greater than the beam divergence, the reflectivities are correspondingly reduced); (3) small strains or thermal-expansion changes can shift the Bragg condition out of the resonance region; (4) because the resonance is so sharp, there is a problem of finding the exact Bragg angle which actually passes the resonance radiation. As has already been demonstrated, these problems are not insurmountable, but it is clearly desirable to have alternative approaches available.

The alternative discussed here is to filter by multiple grazing-incidence reflection from mirrors coated with grazing-incidence antireflection films[1,12,13] in which either the films or substrate contain resonant Mössbauer nuclei. Typically, nonresonant reflectivities can be suppressed to 10^{-4}–10^{-3} while maintaining resonant reflectivities of $\approx 70\%$, with half-widths strongly broadened by "enhancement" to $\Gamma_{\text{eff}} \approx 20\Gamma$. Effective filtering should be possible with three to four reflections, or alternatively, with one to two reflections plus time resolution.

Because this is an index-of-refraction technique, no crystals are needed and the system is freed of the restrictions imposed by a Bragg crystalline condition. As a consequence, the filter can accept the full beam divergence of the synchrotron, and the system is stable against lattice-parameter changes, such as might be caused by heating or radiation damage. Furthermore, the films are relatively easy to fabricate, and the techniques can be applied to a number of low-energy Mössbauer transitions.

Perhaps the most important advantage is that, by using different combinations of films and substrates, the response can be tailored to give narrow resonance widths $\Delta\omega \approx \Gamma$ and corresponding delayed scattering times to optimize time filtering, or at the other extreme, to produce filters of very broad width with $\Delta\omega \approx 100\Gamma$, which would be ideal for a high-resolution x-ray source.

On the negative side, the grazing-incidence geometry is very difficult to work with, and one must contend with small-angle—scattering "noise" which limits the possible signal-to-noise ratio for a single reflection.[14]

The time response itself is of considerable interest and there are several novel aspects: First, there will be "quantum beats" at frequencies Ω_B due to the interference between the radiation emitted by different hyperfine oscillators, so the beat pattern is determined by the hyperfine splitting. Secondly, there are two interesting dynamical effects—first, due to the "enhancement effect" the coherent decay is sped up relative to the natural lifetime for incoherent decay and internal conversion absorption; secondly, there will be "dynamical beats" at frequencies ω_B (superimposed on the quantum-beat spectrum) which qualitatively can be viewed as an interference between the natural "ringing" of an oscillator at its resonance frequency ω_0 and the collective response which rings with a median frequency $\omega_0+\omega_B$. Finally, there is also a multiple-reflection delay to the response, which should be a useful aid for time filtering.

This paper develops the theory for resonant filtering of synchrotron radiation using GIAR films, examining, in particular, the resulting frequency spectrum, the integrated response, and the time response for resonant ^{57}Fe mirrors coated with $\lambda/4$ GIAR films. Alternate thin-film techniques which can be used to tailor the response will be discussed in a future paper.[15]

We have organized this paper as follows: In Sec. II we examine the frequency spectrum and integrated response for a grazing-incidence filter system, and in Sec. III the time response is treated. In Sec. IV we summarize our main conclusions.

II. FREQUENCY SPECTRUM AND INTEGRATED RESPONSE

Synchrotron radiation is a very bright, white source of radiation with fluxes in the 10-keV region approaching 2×10^{12} photons/sec per eV per mrad of Δ_y (see Fig. 1). Future machines are expected to have fluxes several orders of magnitude greater. The radiation is highly collimated about the plane of the synchrotron, with the divergence at 10 keV being $\Delta_x \simeq 0.1$–0.2 mrad, and the radiation is highly linearly polarized, with about 90% of the intensity associated with the component parallel to the plane of the orbit ($\hat{\epsilon}_y$ in Fig. 1). There is also a stable periodic time structure, with the duration of each pulse being $\approx 10^{-10}$ sec, and the separation between pulses, depending on the electron bunching, being $\approx 10^{-6}$ sec for operation in a single-bunch mode.

As we saw in the preceding paper, using an impedance-matched quarter-wave film it is possible to obtain a pure nuclear reflection at grazing incidence, with a resonant re-

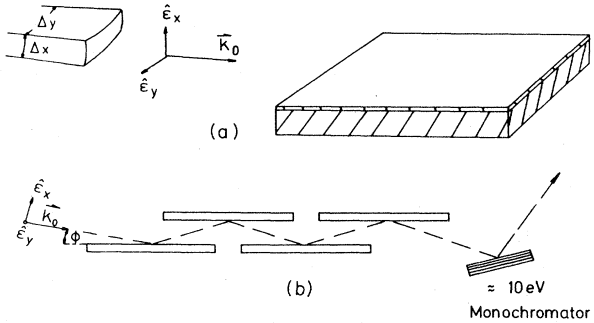

FIG. 1. Schematic of reflection geometry.

flectivity $|R|^2_{res}\approx 0.7$ and a strongly broadened width, $\Gamma_{eff}\approx 20\Gamma$, and with a nonresonant reflectivity $|R|^2_{nonres}\lesssim 10^{-3}$, which is suppressed over approximately a 1-keV region about resonance.

Thus it should be possible to effectively filter the radiation with a threefold to fourfold reflection from a system of parallel mirrors as indicated in Fig. 1(b). The resulting radiation will be "purely resonant" within a $\approx$1-keV region about resonance. Outside this keV region, however, much stronger nonresonant reflection will occur, and to remove this background radiation one broad-bandpass Bragg monochromator is required to restrict the frequency band to, say, $\hbar\Delta\omega_s\approx 10$ eV. (Actually, the Bragg monochromator may not be required if the filtered radiation is to be used for interferometry, or for dynamical γ-ray optics experiments since then a monochromatizing Bragg reflection is contained in the experiment itself.)

As discussed in paper I,[13] there are a large number of possible materials suitable for an impedance-matched quarter-wave film for ^{57}Fe. To be specific, however, we will make most of our calculations for a Te film, for which the optimum parameters are $l_1\approx 76$ Å and $\phi_{min}\approx 4.4$ mrad, and the electronic reflection is suppressed to $|R_e|^2\simeq 9.4\times 10^{-4}$.

The filter system is then taken as a system of m parallel mirrors of ^{57}Fe, each coated with a quarter-wave film of Te. The internal magnetic fields **B** in the separate mirrors will be assumed to be in parallel alignment.

For parallel alignment of the internal fields, the filter system has well-defined eigenpolarizations $\hat{\epsilon}_\eta(\omega)$, $\eta=$I,II which are determined by the resonant ^{57}Fe medium as given explicitly by Eq. (6) of paper III.[1] The eigenpolarizations are generally frequency dependent and nonorthogonal, but as discussed in paper III, for the special cases of $\mathbf{B}||\mathbf{k}_0$, or $\mathbf{B}\perp\mathbf{k}_0$, or if there is no Zeeman splitting, then the bases are orthogonal and frequency independent.

For incident $\hat{\epsilon}_\eta$ *eigenpolarization,* the reflection amplitude of the m mirror filter is

$$R_\eta^{(m)}(\omega,\phi)=\left[\frac{R_{01}(\eta)+R_{12}(\eta)e^{2ig_1(\eta)l_1}}{1+R_{01}(\eta)R_{12}(\eta)e^{2ig_1(\eta)l_1}}\right]^m , \tag{1}$$

where the notation is that of Eq. (17) of paper III. For arbitrary incident polarization, the reflectivity of the filter is then given by

$$|R^{(m)}(\omega,\phi;\hat{\epsilon}_0)|^2=|\tilde{R}^{(m)}\hat{\epsilon}_0|^2 , \tag{2}$$

where the reflection matrix $\tilde{R}^{(m)}$ is given by Eq. (15) of paper III, but with R_I, R_{II} now given by Eq. (1). For the special cases of orthogonal eigenbases, the reflectivity is

$$|R^{(m)}(\omega,\phi;\hat{\epsilon}_0)|^2=\sum_{\eta=I,II}|R_\eta^{(m)}(\omega,\phi)|^2|\hat{\epsilon}_0^*\cdot\hat{\epsilon}_\eta|^2 . \tag{3}$$

For an incident *synchrotron pulse* $I_{0p}(\phi)$ of polarization $\hat{\epsilon}_0$, where $I_{0p}(\phi)$ gives the number of photons/eV per mrad^2 *per pulse* incident on the filter at the angle ϕ, the frequency spectrum of the reflected radiation is (see Appendix A)

$$I^{(m)}(\omega,\phi)=|R^{(m)}(\phi,\omega;\hat{\epsilon}_0)|^2 I_{0p}(\phi) . \tag{4}$$

As discussed in Appendix A, $I^{(m)}(\omega,\phi)$ gives the expected number of photons/eV per mrad^2 in the reflected beam (per pulse) at ϕ at the frequency ω. However, $I(\omega,\phi)$ is not a "steady-state" distribution: it is the frequency distribution obtained in observing for $t\propto 0\rightarrow\infty$ following a pulse excitation at $t=0$. If instead only delayed counts at $t\gtrsim 1/\Gamma$ are observed, then the effective frequency distribution will be narrowed.

The frequency spectrum will depend on the orientation of the internal field **B**, and on the number of reflections in the filter (and, of course, on the quarter-wave film used). In Fig. 2 we plot the near-resonant spectrum for $m=1$–4 reflections for a Te filter with $\mathbf{B}||\mathbf{k}_0$. In this case the eigenpolarizations are the orthogonal right- and left-circularly-polarized bases $\hat{\epsilon}_{(+1)}$ and $\hat{\epsilon}_{(-1)}$. Because the synchrotron source is essentially linearly polarized, the reflectivity is

$$|R^{(m)}(\omega,\phi;\hat{\epsilon}_0)|^2=\tfrac{1}{2}[\,|R_{(+1)}(\omega,\phi)|^{2m}+|R_{(-1)}(\omega,\phi)|^{2m}\,] . \tag{5}$$

The near-resonant spectrum of the eigenbasis reflectivities $|R_{(\pm1)}|^2$ for a single reflection are given in Fig. 4(b) of paper III, which shows one that the peak reflectivities are $|R_{(\pm1)}|^2_{max}\simeq 0.7$. For the reflection of synchrotron radiation, the reflectivities are reduced by $\frac{1}{2}$ because the eigenpolarizations are circular while the synchrotron radiation is essentially linearly polarized. However, after the first reflection in the filter the radiation is circularly polarized: $\hat{\epsilon}_{(+1)}$ near the $M=+1$ resonances and $\hat{\epsilon}_{(-1)}$ near the $M=-1$ resonances. Thus there is no further polarization loss in multiple scattering other than the initial factor of $\frac{1}{2}$.

We also note that the resonances are strongly broadened. This broadening is due to the refraction-augmented enhancement effect as discussed in paper III. However, as we see from Fig. 2, the effect of multiple reflection is to narrow the resonance. In particular, for $m=1$, the half-width of the strongest resonance is $\Gamma'\approx 25\Gamma$, while after three reflections the width is reduced

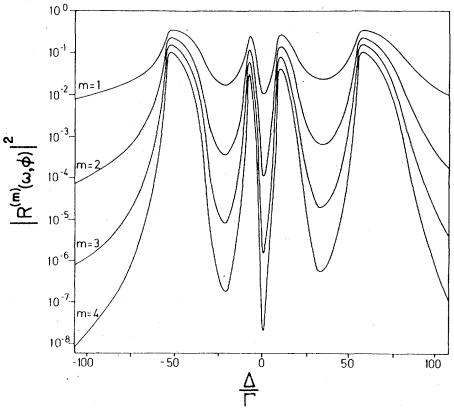

FIG. 2. Near-resonant frequency spectrum of filtered synchrotron radiation, $|R^{(m)}(\omega,\phi)|^2$ vs ω, for m mirror filter system for $m=1$–4. The resonant ^{57}Fe mirrors are each coated with 76 Å of Te, for which the optimum $\phi=4.4$ mrad, and all internal fields are aligned $\mathbf{B}||\mathbf{k}_0$.

to $\Gamma' \approx 9\Gamma$. This sharpening effect of multiple reflection is an immediate consequence of "folding" the single-reflection-resonance spectrum m times.

In Fig. 3 we give the corresponding results for $\mathbf{B}\perp\mathbf{k}_0$ (and for $\mathbf{B}$ parallel to the plane of the film). In this case the eigenpolarizations are the linear $\hat{\epsilon}_\sigma, \hat{\epsilon}_\pi$ bases. The incident synchrotron radiation is approximately 90% $\hat{\epsilon}_\sigma$- and 10% $\hat{\epsilon}_\pi$-polarized. Treating these components as independent, the reflectivity is

$$\langle \mid R^{(m)}(\omega,\phi;\hat{\epsilon}_0) \mid^2 \rangle = 0.9 \mid R_\sigma(\omega,\phi) \mid^{2m} + 0.1 \mid R_\pi(\omega,\phi) \mid^{2m} . \quad (6)$$

The near-resonant spectrum for the eigenbasis reflectivities $\mid R_\sigma \mid^2, \mid R_\pi \mid^2$ are given in Fig. 4(a) of paper III. For this orientation of the B field, the filtered radiation is now linearly polarized: $\hat{\epsilon}_\sigma$ for frequencies near the four $M=\pm 1$ resonances and $\hat{\epsilon}_\pi$ for frequencies near the two $M=0$ resonances. There is now better coupling to the predominantly linearly polarized synchrotron radiation, but this is offset by the fact that the oscillator strengths are weaker for $\mathbf{B}\perp\mathbf{k}_0$ than for $\mathbf{B}\|\mathbf{k}_0$ as we discussed in paper III, and we see from Figs. 2 and 3 that the peak reflectivities and widths are smaller for $\mathbf{B}\perp\mathbf{k}_0$ than for $\mathbf{B}\|\mathbf{k}_0$.

The quantity of real interest in filtering is the integrated response—the total number of resonant (N_n) and nonresonant (N_e) quanta reflected, and the signal-to-noise ratio N_n/N_e. The total integrated flux is given by

$$N^{(m)} = \Delta_y \int_{\Delta_x} d\phi \int_{\Delta\omega_s} d(\hbar\omega)\, I^{(m)}(\omega,\phi) . \quad (7)$$

$N^{(m)}$ gives the expected number of photons reflected per pulse from an m mirror filter system. Here, $\Delta_x\Delta_y$ is the angular collimation of the incident synchrotron pulse ($\Delta_y \approx 1$ mrad, $\Delta_x \approx 0.2$ mrad) and $\hbar\Delta\omega_s$ is the frequency spread of the synchrotron pulse, which, as discussed before, we will take as $\hbar\Delta\omega_s \simeq 10$ eV. The expected number of photons reflected per second is then $n_p N^{(m)}$, where n_p is the number of pulses per second (or, equivalently, we replace I_{0p} by $I_0 = n_p I_{0p}$, which equals the incident photons/eV per sec per mrad^2).

The nonresonant "noise" passed by the filter is then

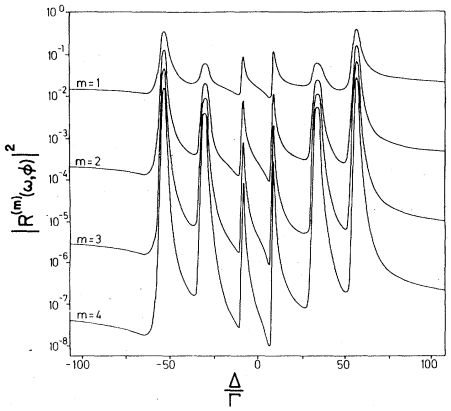

FIG. 3. Near-resonant frequency spectrum of filtered synchrotron radiation for m mirror filter system as in Fig. 2, but now with $\mathbf{B}\perp\mathbf{k}_0$ and $\mathbf{B}$ in plane of film.

$$N_e^{(m)} = \hbar\Delta\omega_s \mid \bar{R}_e \mid^{2m} I_0 \Delta_x \Delta_y , \quad (8)$$

where

$$\mid \bar{R}_e \mid^2 = \Delta_x^{-1} \int_{\Delta_x} \mid R_e(\phi) \mid^2 d\phi$$

is the angle-averaged electronic reflectivity per mirror. $\mid \bar{R}_e \mid^2$ must also be averaged over thickness variations of the quarter-wave film as discussed in paper I.

The resonant "signal" passed is

$$N_n^{(m)} = N^{(m)} - N_e^{(m)} = S_n^{(m)} \hbar\Gamma I_0 \Delta_x \Delta_y , \quad (9)$$

where the "signal factor" $S_n^{(m)}$ of the m mirror filter is given by

$$S_n^{(m)} \cong \Gamma^{-1} \sum_{m_0,M} \Delta\omega^{(m)}(m_0 M) \mid R^{(m)}(m_0 M;\hat{\epsilon}_0) \mid^2_{\max} . \quad (10)$$

Here, $\Delta\omega^{(m)}(m_0 M)$ is the resonance half-width of the m mirror filter for the $m_0 \leftrightarrow m_1 = m_0 + M$ resonance, and $\mid R^{(m)}(m_0 M;\hat{\epsilon}_0) \mid^2_{\max}$ is the peak reflectivity. The signal factor $S_n^{(m)}$ gives the integrated resonant signal passed by the filter in units of $\hbar\Gamma I_0 \Delta_x \Delta_y$, the total number of resonant photons incident per sec on the filter within a *natural* Γ of resonance. We note, however, that because the resonance half-widths $\Delta\omega^{(m)}(m_0 M)$ are strongly broadened over Γ, the "signal factor" $S_n^{(m)}$ can exceed unity.

For convenience of comparing the signal-to-noise ratio, we also introduce the "noise factor"

$$S_e^{(m)} = \Gamma^{-1} \Delta\omega_s \mid \bar{R}_e \mid^{2m} , \quad (11)$$

so that the noise passed is

$$N_e^{(m)} = S_e^{(m)} \hbar\Gamma I_0 \Delta_x \Delta_y .$$

For a Te quarter-wave film, the effective widths and peak reflectivities are given in Fig. 2 for $\mathbf{B}\|\mathbf{k}_0$, and we find that after a threefold reflection, the noise factor is $S_e^{(3)} \simeq 1.7$, while the signal factor is $S_n^{(3)} \simeq 3.6$, giving a signal-to-noise ratio of $S_n^{(3)}/S_e^{(3)} = 2.2$. If the filter is operated instead with $\mathbf{B}\perp\mathbf{k}_0$, as in Fig. 3, then S_n is reduced to $S_n^{(3)} \simeq 2.7$, and we see that after three reflections the enhanced polarization coupling to the synchrotron beam which occurs for $\mathbf{B}\perp\mathbf{k}_0$ is offset by the weaker oscillator strengths. For a fourfold reflection with $\mathbf{B}\|\mathbf{k}_0$, the signal is only reduced to $S_n^{(4)} \simeq 2.1$, while the noise drops to $S_e^{(4)} \simeq 1.6 \times 10^{-3}$, giving a very pure resonance signal, $S_n^{(4)}/S_e^{(4)} \simeq 1.3 \times 10^3$. The filtered radiation will then have four frequency components with relative intensities $\Delta\omega^{(4)} \mid R^{(4)} \mid^2 \simeq 0.80$, 0.08, 0.30, and 1.0, and corresponding widths $\Delta\omega^{(4)} \simeq 6.3\Gamma$, 1.9Γ, 4.7Γ, and 7.8Γ. As we have noted before, the four components are also circularly polarized, the two $M=+1$ resonances being right-circularly-polarized about $+\hat{\mathbf{k}}_0$, and the two $M=-1$ resonances being left-circularly-polarized. We also note again that although "enhancement" gives strongly broadened resonance widths $\Delta\omega(m_0 M) \approx 25\Gamma$ following a single reflection, the sharpening effect of four reflections reduces the widths to $\Delta\omega \approx 8\Gamma$.

III. TIME RESPONSE

An alternative filter technique is "time filtering," first suggested by Ruby.[2] The synchrotron radiation from SPEAR or DORIS operating in the single-bunch mode consists of sharp pulses of about 10^{-9} sec duration and about 10^{-6} sec separation between pulses. Excited nuclear states of energy $\lesssim 100$ keV commonly have lifetimes in the range $\Gamma^{-1}=10^{-9}$–10^{-6} sec. If the pulse impinges upon a sample containing the resonant nuclei, then the electronically scattered x rays, photoelectrons, etc. will emerge promptly during the 10^{-10}-sec pulse, while those processes involving nuclear excitation will be delayed a mean time Γ^{-1}. Therefore, by using a timed detector which can recover from the prompt pulse in a time short compared to Γ^{-1}, the resonant and nonresonant events can be separated temporally. In practice, to avoid detector saturation, it is necessary to use time filtering in conjunction with some form of pure nuclear reflection to suppress the prompt nonresonant pulse.

The time-dependent photon flux following excitation of an m mirror system by a synchrotron pulse of polarization $\hat{\epsilon}_0$ incident at $t_0=0$ is given by (see Appendix A and Ref. 9)

$$I^{(m)}(t,\phi)=[2\pi\hbar I_{0p}(\phi)]\,|\,R^{(m)}(t,\phi;\hat{\epsilon}_0)\,|^2\,, \tag{12}$$

where $R^{(m)}(t,\phi)$ gives the amplitude response to a δ-function pulse,

$$R^{(m)}(t,\phi;\hat{\epsilon}_0)=(1/2\pi)\int_{-\infty}^{+\infty} d\omega\, R^{(m)}(\omega,\phi;\hat{\epsilon}_0)e^{-i\omega t}\,. \tag{13}$$

Here,

$$R^{(m)}(\omega,\phi;\hat{\epsilon}_0)=\tilde{R}^{(m)}(\omega,\phi)\hat{\epsilon}_0$$

is the reflection amplitude of the filter system as given by Eq. (2), and as before, $I_{0p}(\phi)$ is equal to a number of photons/eV per mrad^2 per synchrotron pulse incident at ϕ.

$I(t,\phi)dt\,d\phi\,\Delta_y$ then gives the expected number of photons reflected between t and $t+dt$ in the angular region $d\phi$ about ϕ and Δ_y mrad in the $\hat{\mathbf{y}}$ direction (see Fig. 1). The total integrated flux $N^{(m)}$ of Eq. (7) is then also given by

$$N^{(m)}=\Delta_y\int_{\Delta_x} d\phi\int_0^\infty dt\, I^{(m)}(t,\phi)\,. \tag{14}$$

For the particular cases of orthogonal eigenbasis, $I(t,\phi)$ simplifies to

$$I^{(m)}(t,\phi)=2\pi\hbar I_{0p}(\phi)\sum_{\eta=\mathrm{I,II}}|\,R_\eta^{(m)}(t,\phi)\,|^2\,|\,\hat{\epsilon}_0^*\cdot\hat{\epsilon}_\eta\,|^2\,, \tag{15}$$

where $R_\eta^{(m)}(t,\phi)$ is now the Fourier transform of the eigenpolarization response $R_\eta^{(m)}(\omega,\phi)$ given by Eq. (1). As discussed in paper III, the effect of the impedance-matched quarter-wave film is to effectively remove all electronic scattering, so that, to very good approximation, $R_\eta^{(m)}(\omega,\phi)$ is a pure nuclear reflection,

$$R_\eta^{(m)}(\omega,\phi)\cong\left[\frac{1-\beta_N(\eta)}{1+\beta_N(\eta)}\right]^m, \tag{16}$$

where

$$\beta_N(\eta)=[1+n\lambda^2 f_N(\eta)/\pi(\phi^2-\phi_c^2+in\lambda\sigma_e)]^{1/2}\,. \tag{17}$$

As discussed in paper III, the nuclear scattering amplitude $f_N(\eta)$ is a superposition of oscillators,

$$f_N(\eta)=\sum_{m_0,M} f_0(m_0M;\hat{\epsilon}_\eta)/[x(m_0M)-i]\,, \tag{18}$$

where

$$x(m_0M)=2[E_1(j_1m_0+M)-E_0(j_0m_0)-\hbar\omega]/\Gamma\,,$$

and the oscillator strength of the m_0M resonance for $\hat{\epsilon}_\eta$ eigenpolarization is given by

$$f_0(m_0M;\hat{\epsilon}_\eta)=\frac{2\lambda_0 e^{-k^2\langle x^2\rangle}P}{2j_0+1}\left[\frac{\Gamma_\gamma}{\Gamma}\right]\times C^2(j_0Lj_1;m_0M)\,|\,\hat{\epsilon}_\eta^*\cdot Y_{LM}^{(\lambda)}(\hat{\mathbf{k}}_0)\,|^2\,. \tag{19}$$

Here the notation is that of Eq. (5) of paper III.

A. Isolated resonance: Dynamical effects

We first consider a well-isolated resonance and examine the dynamical effects of enhanced decay, dynamical beats, and multiple-reflection delay. The quantum beats occurring between different resonances will be discussed in the following section.

For a well-isolated resonance with transition frequency $\omega_0(m_0M)$, we take

$$f_N(\eta)=f_0(m_0M;\hat{\epsilon}_\eta)/[x(m_0M)-i]$$

in Eq. (17). With the approximation (16), the integration of Eq. (13) can be carried out analytically as shown in Appendix B, giving (for $t>0$)

$$R_\eta^{(m)}(t,\phi)=(-i)^m e^{-i[\omega_0(m_0M)+\omega_B(m_0M)]t}e^{-\Gamma t/2}m\frac{J_m[\omega_B(m_0M)t]}{t}\,, \tag{20}$$

where J_m is the mth-order cylindrical Bessel function, and the complex dynamical beat frequency is given by

$$\omega_B(m_0M;\phi;\hat{\epsilon}_\eta)\equiv\omega_B'(mM;\phi;\hat{\epsilon}_\eta)-i\omega_B''(mM;\phi;\hat{\epsilon}_\eta)=\pi\lambda^2 n f_0(m_0M;\hat{\epsilon}_\eta)\Gamma/(\phi^2-\phi_c^2+in\lambda\sigma_e)\,. \tag{21}$$

For ^{57}Fe coated with Te ($\phi=4.4\times10^{-3}$ rad) with $\mathbf{B}\|\mathbf{k}_0$, then $\omega_B'\simeq10\Gamma$ and $\omega_B''\simeq1.4\Gamma$ for the strong $M=\pm1$ resonances.

From Eqs. (15) and (20) the time spectrum is then

$$I^{(m)}(t,\phi)=[2\pi\hbar I_{0p}(\phi)]e^{-(\Gamma+\omega_B'')t}\,|\,mJ_m(\omega_B t)\,|^2/t^2\,. \tag{22}$$

For intermediate t, $m(\omega_B')^{-1}<t<m(\omega_B'')^{-1}$, then

$$J_m(z)\sim\sqrt{2/\pi z}\cos(z-\pi/4-m\pi/2)\,,$$

so that

$$I^{(m)}(t,\phi)\sim\frac{e^{-(\Gamma+2\omega_B'')t}}{t^3}\cos^2(\omega_B' t-\pi/4-m\pi/2)\ , \tag{23}$$

while for large t, $t\gg m(\omega_B'')^{-1}$, then

$$I^{(m)}(t,\phi)\sim\frac{e^{-\Gamma t}}{t^3}\ . \tag{23'}$$

From Eqs. (23) and (23') we note first that there is a sped-up nonexponential decay $\exp(-\Gamma t)/t^3$. As discussed before, this is a consequence of the *enhancement effect*:[16] For waves incident near grazing incidence (or Bragg) on a resonant medium, there is a broadened width to the frequency response due to coherent reemission into the reflection channel, and, correspondingly, the time response for coherent scattering is *sped-up* relative to the natural lifetime for incoherent decay and internal conversion absorption. This gives an enhancement of the coherent scattering and consequent suppression of the incoherent processes. As discussed in paper III,[1] enhancement is further augmented by refraction.

Secondly, we see that there are *dynamical beats* in the spectrum at the frequency $\omega_B'(m_0M)$: Again, this is a dynamical effect, and is essentially a competition between the natural "ringing" at ω_0 and the collective response at $\omega_0+\omega_B$. For the case of $\mathbf{B}||\mathbf{k}_0$ and $\phi=4.4\times10^{-3}$ rad, the dynamical beat frequencies are $\omega_B'\simeq10\Gamma$ and 3.3Γ for the strong and weak $M=\pm1$ resonances, giving $\omega_B^{-1}\approx10$ and 30 nsec, and the beats should be observable.

In the absence of photoabsorption ω_B is purely real, $\omega_B=\omega_B'$. However, for the example considered above ω_B'' is appreciable and acts to damp the dynamical beats. For impedance-matched quarter-wave films for which $\phi_0\simeq\phi_c$, then ω_B'' will even be the dominant term ($\omega_B'\to0$ and $\omega_B''\to\sigma_0\Gamma/4\sigma_e$ as $\phi\to\phi_c$) and the beats are completely damped.

Finally, we also note there is a *multiple-reflection delay*: For small t, $t\ll\omega_B^{-1}$, then $J_m(z)\approx z^m/(2^m m!)$, so that

$$I^{(m)}(t,\phi)\approx t^{2m-2}e^{-(\Gamma+2\omega_B'')t}\ . \tag{24}$$

We see that multiple-reflection suppresses the initial response $\propto t^{2m-2}$. This produces a delay in the response, giving a sharper frequency spectrum, in agreement with the discussion in Sec. II.

Qualitatively, the nature of the delayed response from a compound system is clear: Following the initial sharp pulse excitation, the first reflection sends out a delayed, long-coherence-length wave

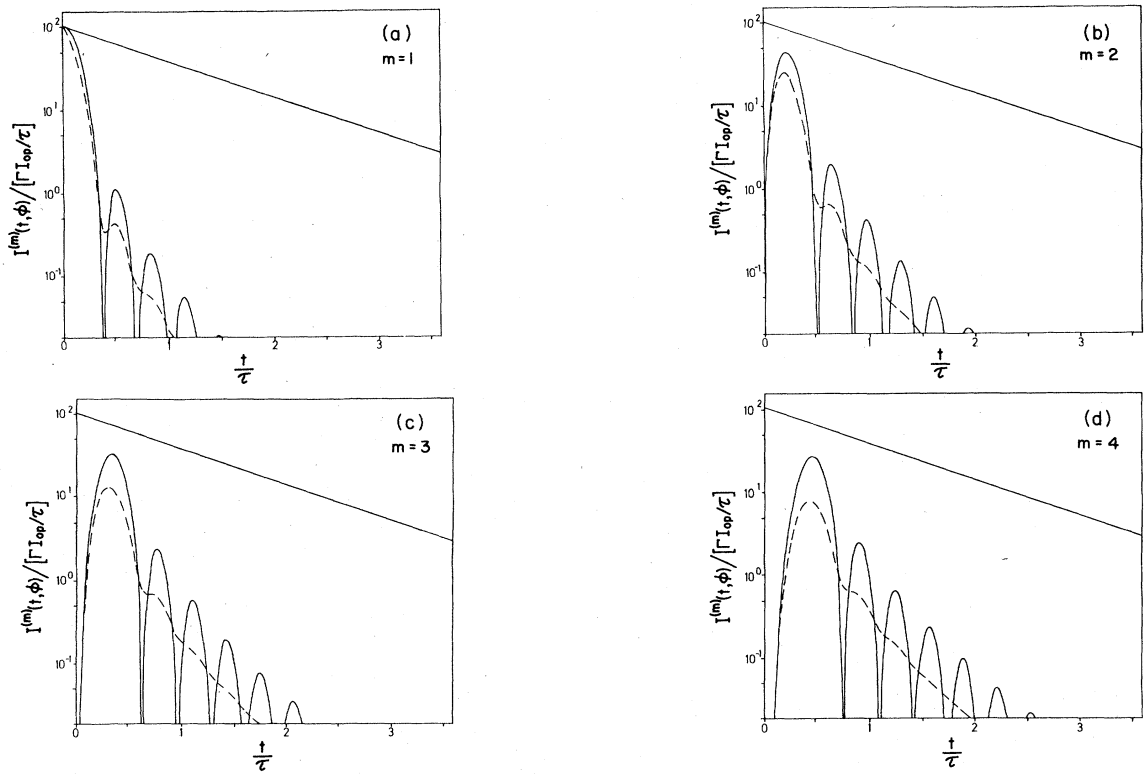

FIG. 4. Time response $I^{(m)}(t,\phi)/(\Gamma I_{0p}/\tau)$ vs t following excitation of m mirror system with a synchrotron pulse for $m=1$–4. The resonant ^{57}Fe mirrors are each coated with 76 Å of Te, so that $\phi=4.4$ mrad, and all internal fields are taken $\mathbf{B}||\mathbf{k}_0$. Here we only include the effects of a single isolated resonance and use the parameters appropriate for the two strong $M=\pm1$ resonances for which $\omega_B\simeq10\Gamma-i\,1.4\Gamma$. The solid oscillating lines give $I^{(m)}(t)$ in the limit $\omega_B''=0$, while the dashed lines include damping. The upper solid lines give the natural decay $\exp(-\Gamma t)$.

$$-i\exp\{-i(\omega_0+\omega_B-i\Gamma/2)t\}J_1(\omega_B t)/t \ .$$

In the second reflection, resonant absorption-reemission of the incident nearly monochromatic wave gives an additional delay $\approx\Gamma_{\rm eff}^{-1}$, where $\Gamma_{\rm eff}^{-1}$ is the effective delay of the collective response, $\Gamma_{\rm eff}^{-1}\approx\omega_B^{-1}$. Speaking classically, the near-resonant incident wave must first build up the oscillations of the resonators in the second film before any appreciable radiation is sent out. Each additional reflection will induce similar delays. Thus the initial response from the compound system is zero, as given explicitly by the t^{2m-2} dependence, with the maximum response occurring only after a delay $\approx(2m-2)\Gamma_{\rm eff}^{-1}$. As noted earlier, the delayed response should be a useful aid for time filtering.

The features of enhanced decay, dynamical beats, and multiple-reflection delay are shown explicitly in Figs. 4 and 5. The solid oscillating lines give $I^{(m)}(t,\phi)$ versus t for $m=1$–4 reflections in the limit of zero photoabsorption damping ($\omega_B''=0$), while the dashed lines include the damping. The upper solid line gives the natural exponential decay $\exp(-\Gamma t)$, normalized to the same initial value as $I^{(1)}(t,\phi)$. In Fig. 4 we have taken the oscillator strength appropriate for the two strong $M=\pm1$ resonances of ^{57}Fe with $\mathbf{B}||\mathbf{k}_0$, $\hat{\epsilon}_\eta=\hat{\epsilon}_{(\pm1)}$, $\phi=4.4\times10^{-3}$ rad, which gives $\omega_B=10\Gamma-i\,1.4\Gamma$. Figure 5 gives the corresponding plots with the oscillator strength of the two weak resonances, so that $\omega_B=3.3\Gamma-i\,0.5\Gamma$.

B. Quantum beats

The dynamical beats discussed above are a dynamical effect occurring for each isolated resonance. A fundamentally more important "quantum-beat" spectrum will be superimposed on the dynamical beats whenever there is splitting of the nuclear levels.[5] The quantum beats are due to the interference between the waves emitted by the various resonances, and hence contain the information of the hyperfine splittings. Of course, for our simple filter, the hyperfine splitting is well known, and our purpose here is to see the exact form of the time spectrum.

The quantum-beat spectrum will be strongly dependent on the orientation of the magnetic field because of the polarization response of the oscillators. Thus, if $\mathbf{B}||\mathbf{k}_0$, then as noted before the eigenpolarizations are circularly polarized, with the $M=+1$ transitions emitting $\hat{\epsilon}_{(+1)}$ radiation, and the $M=-1$ transitions emitting $\hat{\epsilon}_{(-1)}$ radiation. Since there can be no interference between orthogonal polarizations, quantum beats will only arise from the interference between the various $M=+1$ oscillators, and separately from the interference of the $M=-1$ oscillators. For ^{57}Fe there are two $M=+1$ transitions and two $M=-1$ transitions, and since

$$\Delta E(M=+1)=\Delta E(M=-1) \ ,$$

then for $\mathbf{B}||\mathbf{k}_0$ there will be a single beat frequency $\Omega_B=\Delta E\simeq60\Gamma$. [Actually, as discussed below, dynamical

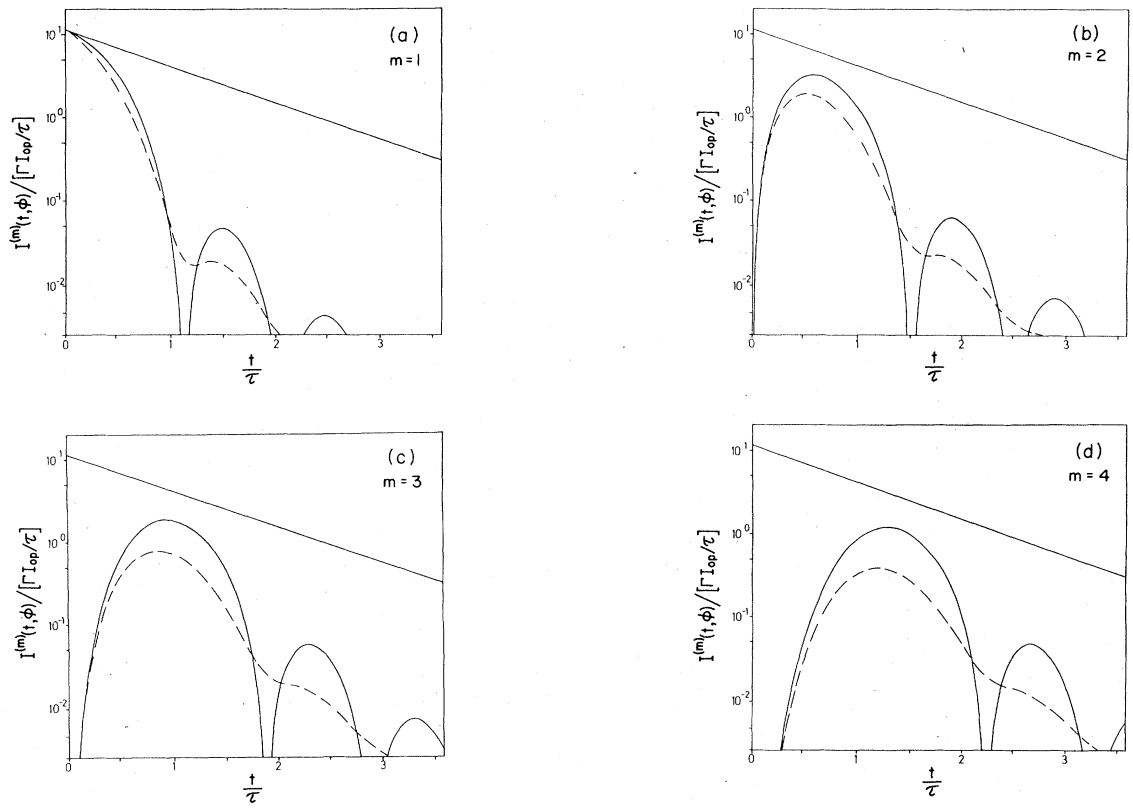

FIG. 5. Time response $I^{(m)}(t,\phi)$ vs t as in Fig. 4, but now with the parameters appropriate for the two weak $M=\pm1$ resonances, for which $\omega_B\simeq3.3\Gamma-i\,0.5\Gamma$, for $m=1$–4 reflections.

effects produce shifts, so that two different beat frequencies $\Omega_B(\pm 1)$ will be observed.] On the other hand, if $\mathbf{B}\perp\mathbf{k}_0$, then the four $M=\pm 1$ oscillators all emit linear $\hat{\epsilon}_\sigma$ radiation, producing four beat frequencies, while the two $M=0$ transtions emit linear $\hat{\epsilon}_\pi$ radiation, producing a single beat frequency. The quantum-beat spectrum is then a superposition of four *unique* frequencies (increased to seven by dynamical shifts).

Noting that the quantum-beat frequencies are much larger than the dynamical beat frequencies, we have (correct to terms of order ω_B/Ω_B), for $\mathbf{B}||\mathbf{k}_0$,

$$I^{(m)}(t,\phi)=\tfrac{1}{2}[\,|R^{(m)}_{(+1)}(t,\phi)|^2 + |R^{(m)}_{(-1)}(t,\phi)|^2][2\pi\hbar I_{0p}] \tag{25}$$

where for $M=\pm 1$,

$$R^{(m)}_M(t,\phi)\approx(-i)^m\sum_{m_0} e^{-i[\omega_0(m_0M)+\omega_B(m_0M)]t} \times e^{-\Gamma t/2} m J_m[\omega_B(m_0M)t]/t\ . \tag{26}$$

For ^{57}Fe with $M_0=\pm\frac{1}{2}$ we see from Eq. (26) that rather than a single quantum-beat frequency Ω_B, dynamical shifts will produce two distinct beat frequencies for $M=\pm 1$,

$$\Omega_B(\pm 1)=\Delta\omega_0(\pm 1)+\Delta\omega'_B(\pm 1)\ . \tag{27}$$

For pure ^{57}Fe, $\Delta\omega_0(\pm 1)\simeq 60\Gamma$, while $\Delta\omega'_B(\pm 1)\simeq\mp 6.8\Gamma$, giving $\Omega_B(+1)\simeq 53.2\Gamma$ for the $M=+1$ resonances and $\Omega_B(-1)\simeq 66.8\Gamma$ for the $M=-1$ resonances. This splitting is obvious in Fig. 4(b) of paper III, which shows that due to the frequency asymmetry of the response about each resonance, the median responses of the $M=+1$ resonances lie closer together than the $M=-1$ resonances.

As given by Eq. (25), the total time-dependent spectrum for ^{57}Fe is a superposition of the two dynamical beat terms $J_m(10\Gamma t)^2$ and $J_m(3.3\Gamma t)^2$, which are plotted in Figs. 4 and 5, and the quantum-beat interference term

$$\{\cos[\Omega_B(+1)t]+\cos[\Omega_B(-1)t]\}J_m(10\Gamma t)J_m(3.3\Gamma t)\ .$$

This response is shown in Fig. 6(a) for a triple reflection from Te-coated mirrors. Here the solid line gives the response time averaged over the rapid quantum-beat oscillations, while the two dashed lines give the upper and lower envelopes with the quantum-beat term included. The actual spectrum then oscillates as

$$\tfrac{1}{2}\{\cos[\Omega_B(+1)t]+\cos[\Omega_B(-1)t]\}$$

between the two envelopes. In Fig. 6(b) we give the corresponding results for a double reflection from Se-coated mirrors. Here the dynamical beats are slower ($\omega_B\simeq 2.0\Gamma$ and 0.7Γ) because of the larger incidence angle $\phi\simeq 6.0\times 10^{-3}$ rad.

If the internal field is rotated so that $\mathbf{B}\perp\mathbf{k}_0$, with $\mathbf{B}$ in the plane of the film, then the time spectrum is changed to

$$I^{(m)}(t,\phi)=[0.9\,|R^{(m)}_\sigma(t,\phi)|^2 + 0.1\,|R^{(m)}_\pi(t,\phi)|^2][2\pi\hbar I_{0p}]\ , \tag{28}$$

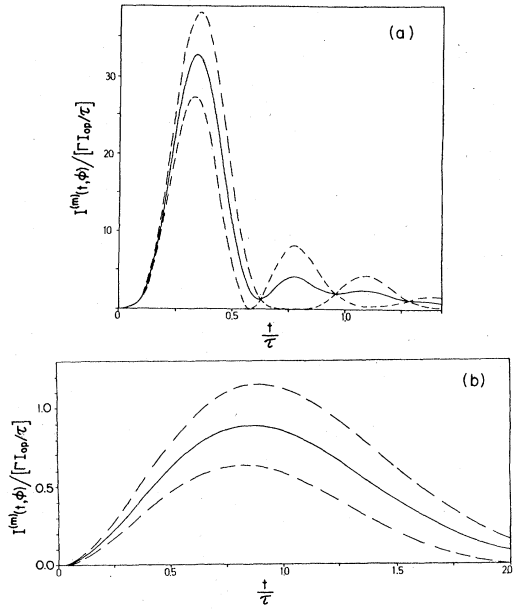

FIG. 6. Time response following excitation by synchrotron-radiation pulse for ^{57}Fe mirror system: (a) Te films, $\phi=4.4$ mrad, $\mathbf{B}||\mathbf{k}_0$, $m=3$; (b) Se films, $\phi=6.0$ mrad, $\mathbf{B}||\mathbf{k}_0$, $m=2$. The solid lines give the response time averaged over the rapid quantum-beat oscillations Ω_B, while the dashed lines give the envelopes produced by the quantum beats.

where

$$R^{(m)}_\sigma\approx(-i)^m\sum_{m_0}\sum_{M=\pm 1} e^{-i[\omega_0(m_0M)+\omega_B(m_0M)]t} \times m J_m[\omega_B(m_0M)t]/t\ ,$$
$$R^{(m)}_\pi\approx(-i)^m\sum_{m_0} e^{-i[\omega_0(m_00)+\omega_B(m_00)]t} \times m J_m[\omega_B(m_00)t]/t\ . \tag{29}$$

Because of the reduced oscillator strengths, the dynamical beat frequencies are now (for ^{57}Fe, $\phi=4.4\times 10^{-3}$ rad) $\omega'_B(\pm 1;\sigma)=4.8\Gamma$ and 1.6Γ for the strong and weak $M=\pm 1$ resonances, and $\omega'_B=6.8\Gamma$ for the $M=0$ transitions. As noted before, the $\hat{\epsilon}_\sigma$ radiation is a superposition of the four $M=\pm 1$ resonances, which, including the dynamical shifts, produce six distinct beat frequencies Ω_B, and the $\hat{\epsilon}_\pi$ radiation is produced by the two $M=0$ resonances, introducing a seventh beat frequency $\Omega_B(0)$.

IV. SUMMARY

This paper has developed the theory for resonant filtering of synchrotron radiation using grazing-incidence antireflection films, examining, in particular, the resulting frequency spectrum, the integrated response, and the time response. As our example case, we have taken resonant mirrors coated with nonresonant $\lambda/4$ quarter-wave films. With alternative mirror systems, such as discussed in paper V,[15] the detailed response can vary, but the general features discussed here persist.

The most important points are the following: In a single reflection, nonresonant reflectivities can typically be suppressed to $\approx 10^{-4}$–10^{-3} while maintaining resonant reflectivities of $\gtrsim 0.7$, with half-widths strongly broadened by enhancement to $\gtrsim 20\Gamma$. It should then be possible to achieve effective filtering by multiple reflection from two to four mirrors, or alternatively, with one to two reflections plus time resolution.

Operated in a single-bunch mode with time resolution, there will be the interesting time aspects of quantum beats exhibiting hyperfine splitting, superimposed dynamical beats occurring for each isolated resonance, and sped-up coherent decay due to the enhancement effect. Also, the effect of multiple reflections will be to induce time delays, corresponding to the width-sharpening effect of multiple reflections. The delayed *peak* response of multiple reflections, in contrast to the prompt peak response of a single reflection, should be a useful feature for signal detection in time-filtering experiments.

A particularly important feature of these mirror filters is that the response can be varied. For example, by using Se rather than Te as the $\lambda/4$ coating for the ^{57}Fe mirror, the widths are decreased by a factor of ≈ 5, giving a sharper resonance signal, and correspondingly, a longer time delay. More generally, by using different combinations of films and substrates as discussed in paper V,[15] the response can be tailored to give narrow resonance widths $\Delta\omega \approx \Gamma$ and long delay times, or at the other extreme, to produce filters of broad width with $\Delta\omega \approx 100\Gamma$. Also, even for a given system, the response can be strongly altered by simply rotating the **B** field from $\mathbf{B}\|\mathbf{k}_0$ to $\mathbf{B}\perp\mathbf{k}_0$.

Because this is an index-of-refraction technique, no crystals are needed and the system is freed of the severe restrictions imposed by a Bragg condition. As a consequence, the filter can accept the full beam divergence of the synchrotron, and the system is stable against lattice-parameter changes, such as might be caused by heating or radiation damage. Because of the high resonant reflectivities and strongly broadened frequency response, grazing-incidence filters offer potentially brighter sources than Bragg filters. Furthermore, the films are relatively easy to fabricate, and the techniques can be applied to a number of low-energy Mössbauer transitions. On the negative side, the grazing-incidence geometry is difficult to work with, and one must contend with small-angle-scattering "noise" which limits the possible signal-to-noise ratio for a single reflection.

ACKNOWLEDGMENTS

This work was partially supported by grants from the National Science Foundation (No. DMR-80-15706) and the Deutsche Forschungsgemeinschaft and the Bundesministerium für Forschung und Technologie (No. 05269GU), Federal Republic of Germany.

APPENDIX A

The incident synchrotron pulse from a single electron is a packet of spread $\Delta\Omega(\phi_0) \approx (0.1 \text{ mrad})^2$, centered at grazing incidence angle ϕ_0 (the Δ_y "fan" in Fig. 1 is produced by the continuous emission of such packets as the electron traverses its circular orbit).

For an incident pulse

$$\mathbf{A}^0(\mathbf{r},t;\phi_0)=(2\pi)^{-1}\int_{-\infty}^{+\infty} d\omega \int_{\Delta\Omega(\phi_0)} d\Omega\, \mathbf{A}^0(\hat{\mathbf{k}}_0,\omega)\exp[i(\mathbf{k}_0\cdot\mathbf{r}-\omega t)] ,$$

the reflected $(\mathbf{k},\omega)$ amplitude is

$$\mathbf{A}^s(\hat{\mathbf{k}},\omega)=\tilde{R}(\omega,\phi)\mathbf{A}^0(\hat{\mathbf{k}}_0,\omega) , \tag{A1}$$

where ϕ is the grazing angle of incidence of $\mathbf{k}_0, \mathbf{k}=(\mathbf{k}_{0xy}, -k_{0z})$, and $\tilde{R}(\omega,\phi)$ is the grazing incidence reflection matrix. The origin of the coordinate system is taken on the surface of the mirror. The time dependent scattered wave is then given by

$$\mathbf{A}^s(\mathbf{r},t;\phi)=(2\pi)^{-1}\int_{-\infty}^{+\infty} d\omega \int_{\Delta\Omega(\phi_0)} d\Omega\, \tilde{R}(\omega,\phi)\mathbf{A}^0(\hat{\mathbf{k}}_0,\omega)\exp[(\mathbf{k}\cdot\mathbf{r}-\omega t)] . \tag{A2}$$

Alternatively, letting

$$\mathbf{A}^0(\hat{\mathbf{k}}_0,\omega)=\int d\omega' \mathbf{A}^0(\hat{\mathbf{k}}_0,\omega')\delta(\omega'-\omega)$$

and taking

$$\delta(\omega'-\omega)=(2\pi)^{-1}\int_{-\infty}^{+\infty} dt'\exp[-i(\omega'-\omega)t'] ,$$

the time-dependent reflected wave at the detector is

$$\mathbf{A}^s(\mathbf{r},t;\phi_0)=\int_{-\infty}^{+\infty} dt'\tilde{R}(t^*-t',\phi_0)\mathbf{A}^0(0,t';\phi_0) . \tag{A3}$$

Here $\mathbf{A}^0(0,t';\phi_0)$ is the pulse incident on the mirror, $t^*=t-r/c$ is the retarded time at the detector, and $\tilde{R}(t^*-t',\phi_0)$ is the amplitude (matrix) of the reflected wave at time t^*-t' due to a δ-function pulse incident at t',

$$\tilde{R}(t^*-t',\phi_0)=(2\pi)^{-1}\int_{-\infty}^{+\infty} d\omega\, \tilde{R}(\omega,\phi_0) \times\exp[-i\omega(t^*-t')] . \tag{A4}$$

In going from Eq. (A2) to (A3), we also made use of the fact that for a grazing incidence nuclear reflection, $\tilde{R}(\omega,\phi)\approx\tilde{R}(\omega,\phi_0)$ for all ϕ in $\Delta\Omega(\phi_0)$, and $\mathbf{k}\cdot\mathbf{r}\approx kr$ in the specularly reflected beam at the detector.

From the scattered photon potential $\mathbf{A}^s$, the time-

dependent scattered flux ($\mathrm{cm}^{-2}\mathrm{sec}^{-1}$) at the detector is given by[17,18]

$$I(t,\phi)=\frac{\omega_0}{2\pi\hbar c}\,|\,\mathbf{A}^s(r,t;\phi)\,|^2\,, \tag{A5}$$

and the frequency spectrum ($\mathrm{cm}^{-2}\mathrm{eV}^{-1}$) is

$$I(\omega,\phi)=\frac{\omega_0}{4\pi^2\hbar^2 c}\,|\,\mathbf{A}^s(r,\omega;\phi)\,|^2\,. \tag{A6}$$

Here ω_0 is the nuclear resonance frequency, and it is assumed that the frequency spread $\Delta\omega$ of the packet is $\ll\omega_0$. This condition holds for both the reflected pulse ($\Delta\omega/\omega_0\leq 100\Gamma/\omega_0\approx 10^{-10}$) and for the premonochromized incident pulse ($\Delta\omega/\omega_0\leq 10^{-3}$). The radiation diverges from the source electron, and multiplying through by the source-detector (distance),^{2} the fluxes will be $\mathrm{rad}^{-2}\mathrm{sec}^{-1}$.

As discussed in Refs. 5 and 9, the synchrotron pulse consists of many photons emitted by the many electrons in the bunch incoherently, one with the other. The pulse from a given electron has a duration $\approx\lambda_c/c\approx 10^{-19}$ sec, or, if this radiation is filtered to about 1 eV, the coherence time becomes $\approx 10^{-15}$ sec, which is still generally very short compared to the response time of $|\,R(t,\phi)\,|^2$ [the shortest response time of $|\,R\,|^2$ is $\approx(100\Gamma)^{-1}\gg 10^{-15}$ sec, which occurs for resonant damping-stabilized films]. The duration of the entire pulse depends on the bunching of the electrons and is typically $\approx 10^{-10}$ sec. The scattered flux should then be computed starting from Eq. (A3), where $\mathbf{A}^0(t)$ represents a *one-photon* amplitude of duration on the order of the coherence time T_c. Since

$$\exp[i\omega_0(t-t')]\widetilde{R}(t-t')\sim\exp[-i(\omega_B-i\Gamma/2)(t-t')]$$

develops slowly relative to the coherence time [here ω_B is the dynamical beat frequency given by Eq. (21)], and since $\mathbf{A}^0(0,t';\phi_0)$ is only nonzero during $t'\approx 0\rightarrow T_c$, then (A3) gives

$$\begin{aligned}\mathbf{A}^s(r,t;\phi_0)&\approx\widetilde{R}(t^*,\phi_0)\int_{-\infty}^{+\infty}dt'\exp(i\omega_0 t')\mathbf{A}^0(0,t';\phi_0)\\&=\widetilde{R}(t^*,\phi_0)\mathbf{A}^0(0,\omega_0;\phi_0)\,.\end{aligned}$$

Furthermore, it will usually be true that the response of $\widetilde{R}$ is also slow relative to the duration of the synchrotron pulse. Then, effectively all single-photon packets are incident at $t_0=0$, and the total reflected flux is simply the single-photon result summed over all photons occurring in the bunch, which just amounts to multiplying by the number of photons in the pulse, and we obtain

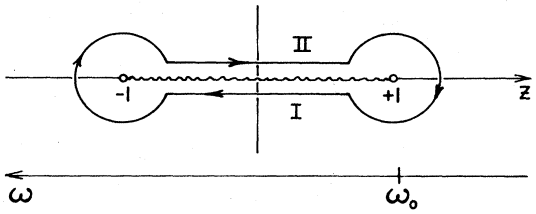

FIG. 7. Branch cut and contour for the integral of Eq. (B4). The phase of $z-1$ is $-\pi$ along both paths I and II, while the phase of $z+1$ is zero along path I and -2π along path II.

$$I(t,\phi)=\sum_{\mu=x,y}[2\pi\hbar I_{0\mu}(\phi)]\,|\,\widetilde{R}(t^*,\phi)\cdot\hat{\epsilon}^0_\mu\,|^2\,. \tag{A7}$$

Here, $I_{0\mu}$ is the number of photons/eV per mrad^2 per synchrotron pulse incident on the crystal at the rocking angle ϕ, with polarization $\hat{\epsilon}^0_\mu$, at frequency ω_0. $I(t,\phi)dt\,d\phi\,\Delta_y$ gives the expected number of photons reflected between t to $t+dt$ in the angular region $d\phi$ about ϕ, and Δ_y mrad in the $\hat{\mathbf{y}}$ direction (see Fig. 1). Alternatively, if the duration of the incident synchrotron pulse is appreciable relative to the characteristic development time of $|\,R(t)\,|^2$, then the response must be folded over the incident pulse shape $P_0(t)$,

$$\begin{aligned}I(t,\phi)=&\sum_{\mu=x,y}[2\pi\hbar I_{0\mu}(\phi)]\\&\times\int dt_0\,|\,\widetilde{R}(t^*-t_0,\phi)\cdot\hat{\epsilon}^0_\mu\,|^2P_0(t_0)\,.\end{aligned} \tag{A8}$$

Similarly, from Eqs. (A1) and (A6), we obtain the frequency distribution,

$$I(\omega,\phi)=\sum_{\mu=x,y}|\,\widetilde{R}(\omega,\phi)\cdot\hat{\epsilon}^0_\mu\,|^2I_{0\mu}(\phi)\,. \tag{A9}$$

$I(\omega,\phi)$ gives the expected number of photons/eV per mrad^2 in the reflected beam (per pulse) at ϕ at the frequency ω. Of course, $I(\omega,\phi)$ is not a steady-state distribution: it is the frequency distribution obtained in observing for $t=0\rightarrow\infty$ following a pulse excitation at $t=0$. If instead only delayed counts at $t\gtrsim 1/\Gamma$ are observed, then the effective frequency distribution will be narrowed.

Of particular interest is the integrated intensity,

$$\begin{aligned}N&=\Delta_y\int_{\Delta_x}d\phi\int_{-\infty}^{+\infty}d(\hbar\omega)I(\omega,\phi)\\&=\Delta_y\int_{\Delta_x}d\phi\int_{-\infty}^{+\infty}dt\,I(t,\phi)\,.\end{aligned} \tag{A10}$$

N gives the expected number of photons reflected per pulse in the angular region $\Delta_x\Delta_y$, and the expected number of photons reflected per second is then n_pN, where n_p is the number of pulses per second.

APPENDIX B

Here we derive Eq. (20): For an *isolated resonance,* the m mirror reflection amplitude given by Eq. (16) can also be written as

$$R^{(m)}(\omega,\phi)=(-1)^m[z-(z^2-1)^{1/2}]^m\,, \tag{B1}$$

where

$$z=\frac{\Gamma}{2\omega_B}\left[\frac{2}{\Gamma}(\omega_0-\omega)-i\right]+1\,, \tag{B2}$$

with ω_B defined by Eq. (21). Thus $R(\omega,\phi)$ has branch points at $z=\pm 1$.

The time-dependent amplitude $R(t,\phi)$ is then given by

$$R^{(m)}(t,\phi)=(1/2\pi)\int_{-\infty}^{+\infty} R^{(m)}(\omega,\phi)e^{-i\omega t}d\omega$$
$$=(2\pi)^{-1}(-1)^{(m+1)}\omega_B\exp[-i(\omega_0+\omega_B-i\Gamma/2)t]\int_C [z-(z^2-1)^{1/2}]^m\exp(i\omega_B tz)dz\ . \quad \text{(B3)}$$

There are two Riemann sheets associated with the branch points, and the correct sheet is determined by $\mathrm{Im}\beta(\omega)>0$ on the real ω axis. For $t>0$, the integration path can be deformed to the contour around the branch cut as shown in Fig. 7 and the contour integral reduces to

$$\int_C (z-\sqrt{z^2-1})^m e^{i\omega_B tz}dz=\int_{-1}^{+1}[(z-i\sqrt{1-z^2})^m-(z+i\sqrt{1-z^2})^m]e^{i\omega_B tz}dz\ . \quad \text{(B4)}$$

Letting $z=\cos\alpha$ then gives

$$\left[-i\int_0^{\pi}\cos[(m-1)\alpha]e^{i\omega_B t\cos\alpha}d\alpha+i\int_0^{\pi}\cos[(m+1)\alpha]e^{i\omega_B t\cos\alpha}d\alpha\right]$$
$$=-(i)^m\pi[J_{m-1}(\omega_B t)+J_{m+1}(\omega_B t)]=-(i)^m 2\pi m J_m(\omega_B t)/(\omega_B t)\ . \quad \text{(B5)}$$

Combining (B5) with (B3) gives Eq. (20). A similar result holds for nuclear Bragg reflections.[9] For $t<0$, the contour is completed in the opposite half plane, $\mathrm{Im}(\omega)>0$, giving $R(t<0)=0$.

[1]J. P. Hannon, G. T. Trammell, M. Mueller, E. Gerdau, H. Winkler, and R. Rüffer, preceding paper Phys. Rev. B **32**, 6363 (1985) (paper III).

[2]S. L. Ruby, J. Phys. (Paris) **35**, C6-209 (1974).

[3]R. L. Mössbauer, Proceedings of the International Union of Crystallography, Madrid, April, 1974 (unpublished), p. 463.

[4]G. T. Trammell, J. P. Hannon, S. L. Ruby, Paul Flinn, R. L. Mössbauer, and F. Parak, in *Workshop on New Directions in Mössbauer Spectroscopy (Argonne, 1977)*, edited by G. J. Perlow (AIP, New York, 1978), pp. 46–49 (AIP Conf. Proc. No. 38).

[5]G. T. Trammell and J. P. Hannon, Phys. Rev. B **18**, 165 (1978).

[6]R. L. Cohen, G. L. Miller, and K. W. West, Phys. Rev. Lett. **41**, 381 (1978).

[7]G. N. Kulipanov and A. N. Skrinskii, Usp. Fiz. Nauk **122**, 369 (1977) [Sov. Phys.—Usp. **20**, 559 (1977)].

[8]A. N. Artern'ev, G. N. Kulipanov, and E. P. Stepanov, Institute of Nuclear Physics (Novosibirsk), Report No. 77-106 (1977) (unpublished).

[9]Yu. M. Kagan, A. M. Afanas'ev, and V. G. Kohn, Phys. Lett. **68A**, 339 (1978); J. Phys. C **12**, 615 (1979).

[10]A. I. Chechin, N. V. Andronova, M. V. Zelepurkhin, A. N. Artem'ev, and E. P. Stepanov, Zh. Eksp. Teor. Fiz. Pis'ma Red **37**, 531 (1983) [JETP Lett. **37**, 633 (1983)].

[11]E. Gerdau, R. Rüffer, H. Winkler, W. Tolksdorf, C. P. Klages, and J. P. Hannon, Phys. Rev. Lett. **54**, 835 (1985).

[12]J. P. Hannon, G. T. Trammell, M. Mueller, E. Gerdau, H. Winkler, and R. Rüffer, Phys. Rev. Lett. **43**, 636 (1979).

[13]J. P. Hannon, Nguyen Hung, G. T. Trammell, E. Gerdau, M. Mueller, R. Rüffer, and H. Winkler, Phys. Rev. B **32**, 5068 (1985); **32**, 5081 (1985) (papers I and II).

[14]J. P. Hannon, J. T. Hutton, G. T. Trammell, E. Gerdau, R. Rüffer (unpublished) (paper VI).

[15]J. P. Hannon, J. T. Hutton, N. H. Hung, G. T. Trammell, E. Gerdau, and R. Rüffer (unpublished) (paper V).

[16]G. T. Trammell, in *Chemical Effects on Nuclear Transformations* (International Atomic Energy Agency, Vienna, 1961), Vol. I, p. 75.

[17]J. P. Hannon and G. T. Trammell, Phys. Rev. **169**, 315 (1968).

[18]J. P. Hannon, N. J. Carron, and G. T. Trammell, Phys. Rev. B **9**, 2791 (1974); **9**, 2810 (1974).